Formation of dispersions using "flow focusing" in microchannels

Shelley L. Anna, Nathalie Bontoux,[a) and Howard A. Stone[b)
Division of Engineering and Applied Sciences, Harvard University, Cambridge, Massachusetts 02138

A flow-focusing geometry is integrated into a microfluidic device and used to study drop formation in liquid–liquid systems. A phase diagram illustrating the drop size as a function of flow rates and flow rate ratios of the two liquids includes one regime where drop size is comparable to orifice width and a second regime where drop size is dictated by the diameter of a thin "focused" thread, so drops much smaller than the orifice are formed. Both monodisperse and polydisperse emulsions can be produced. © *2003 American Institute of Physics.* [DOI: 10.1063/1.1537519]

Droplets of one fluid in a second immiscible fluid are useful in a wide range of applications, particularly when the droplet size and the size distribution can be prescribed on a micro- or nanoscale. As examples, many personal care products, foods,[1] and products for topical delivery of drugs are emulsions, and nanoemulsions have been proposed for decontamination of surfaces infected in some way (e.g., bacteria, bioterror agents, etc.).[2] Similar emulsion structures are considered for organizing liquid-crystal droplets into optical devices.[3,4] In this letter, we consider a flow-focusing configuration in a microfluidic device for the formation of both monodisperse and polydisperse emulsions and we qualitatively illustrate aspects for controlling the drop size and distribution as the flow rates of the two liquid phases are varied.

Emulsification methods are plentiful, but most involve mixing two liquids in bulk processes, and many use turbulence to enhance drop breakup. In these "top-down" approaches to emulsification, little control over the formation of individual droplets is available, and a broad distribution of sizes is typically produced.[5] Alternatively, a "bottom-up" approach can be used for emulsification at the level of individual drops. Microfluidic devices are ideal for thinking about this approach to microstructure formation.[6] For example, Thorsen *et al.* formed emulsions in a microfluidic device by colliding an oil stream and a water stream at a T-shaped junction.[7] The resulting drops varied in size depending on the flow rate in each stream. Similar microfluidic approaches to emulsification and two-phase flows have been described elsewhere.[8–12] Alternatively, Gañán-Calvo and Gordillo produced highly monodisperse gas bubbles, less than 100 μm in diameter,[11] using a technique called capillary flow focusing: gas is forced out of a capillary tube into a bath of liquid, the tube is positioned above an orifice, and the pressure-driven contraction flow of the external liquid through the orifice focuses the gas into a thin jet, which subsequently breaks into equal-sized bubbles. In a separate experiment, this geometry was used to produce liquid droplets in air.[13] Bubbles and drops formed by this flow-focusing technique are typically smaller than the upstream capillary tube and vary in size with the flow rates.

In the present study, we report experiments using a flow-focusing geometry, integrated into a planar microchannel design using soft lithography fabrication methods,[14] to form liquid drops in a continuous phase of a second immiscible liquid. Such fabrication methods allow rapid production of an integrated microchannel prototype in essentially a single step.[15] Using oil as the continuous phase and water as the dispersed phase, we observe a wide range of drop formation patterns, depending on the flow rates applied to each liquid inlet stream. We quantify the variation in size of the resulting water drops as a function of the oil flow rate, Q_o, and the ratio of the internal water flow rate to the external oil flow rate, Q_i/Q_o. Both monodisperse and polydisperse patterns of drop formation occur, and the drop size can be either approximately independent of, or strongly dependent on, the flow rates, depending on the operating parameters chosen.

Figure 1 shows the flow-focusing geometry implemented in a microfluidic device: a liquid flows into the middle channel and a second immiscible liquid flows into the two outside channels. The two liquid phases are then forced to flow through a small orifice that is located downstream of the three channels. The outer fluid exerts pressure and viscous stresses that force the inner fluid into a narrow thread, which then breaks inside or downstream of the orifice. In the experiments reported here, the inner fluid is distilled water and
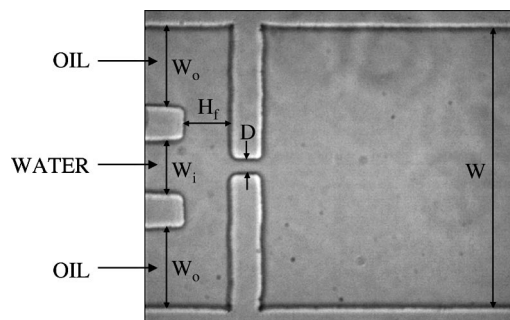

FIG. 1. Flow-focusing geometry implemented in a microfluidic device. An orifice is placed a distance $H_f = 161$ μm downstream of three coaxial inlet streams. Water flows in the central channel, $W_i = 197$ μm, and oil flows in the two outer channels, $W_o = 278$ μm. The total width of the channel is $W = 963$ μm and the width of the orifice is $D = 43.5$ μm. The thickness of the internal walls in the device is 105 μm; this thickness is necessary in order to obtain a uniform seal between the glass cover slip and the poly-(dimethylsiloxane) (PDMS). The uniform depth of the channels is 117 μm. The "design" dimensions were slightly different than the measured values reported here since silicone oil swells the PDMS.

[a)École Polytechnique, Palaiseau, Paris, France.
[b)Electronic mail: has@deas.harvard.edu

Appl. Phys. Lett., Vol. 82, No. 3, 20 January 2003

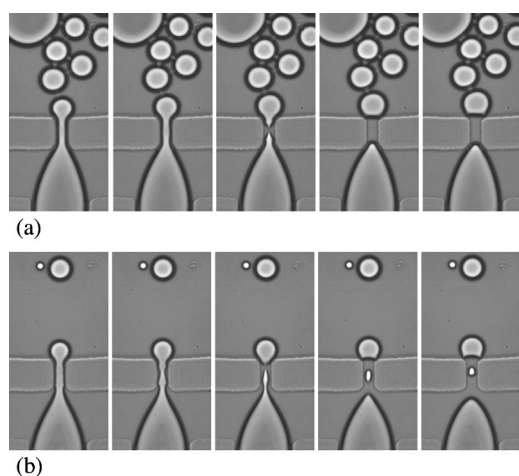Anna, Bontoux, and Stone   365

FIG. 2. Experimental images of drop breakup sequences occurring inside the flow-focusing orifice. (*a*) Uniform-sized drops are formed without visible satellites; breakup occurs inside the orifice. The time interval between images is 1000 μs; $Q_o = 8.3 \times 10^{-5}$ mL/s and $Q_i/Q_o = 1/4$. (*b*) A small satellite accompanies each large drop; breakup occurs at two corresponding locations inside the orifice. The time interval between images is 166 μs; $Q_o = 4.2 \times 10^{-4}$ mL/s and $Q_i/Q_o = 1/40$.

the outer fluid is silicone oil (viscosity, 6 mPa s), which leads to water drops that form in a continuous phase of oil. Span 80 surfactant (Sorbitan monooleate, Aldrich) is dissolved in the oil phase at 0.67 wt %. The surfactant solution was prepared by mechanically mixing the two components for ap-

proximately 30 min and then filtering to eliminate aggregates and prevent clogging of the microchannel.

The fluids are introduced into the microchannel through flexible tubing and the flow rate is controlled using separate syringe pumps for each fluid. In the experiments reported here, the flow rate of the outer fluid (oil), Q_o, is always greater than the flow rate of the inner fluid (water), Q_i. Three different flow rate ratios are chosen, $Q_i/Q_o = 1/4$, 1/40, and 1/400, where the oil flow rate given corresponds to the total flow rate for both oil inlet streams. For each Q_i/Q_o, oil flow rates spanning more than two orders of magnitude are chosen (4.2×10^{-5} mL/s $\leq Q_o \leq 8.3 \times 10^{-3}$ mL/s). At each value of Q_o and Q_i, drop formation is visualized using an inverted microscope and a high-speed camera.

In Fig. 2(a) we show formation of a nearly monodisperse suspension of water droplets with diameter comparable to the orifice width. Breakup occurs within the orifice. In addition, drops may break within the orifice such that one or more satellite droplets are formed in a regular and reproducible manner. Figure 2(b) illustrates this kind of breakup process, which thus naturally forms a bidisperse suspension.

We have conducted many experiments documenting the formation of two-phase liquid–liquid dispersions in microchannels fabricated with the flow-focusing configuration. A phase diagram indicating the range of responses we have observed is shown in Fig. 3. We observe the formation of
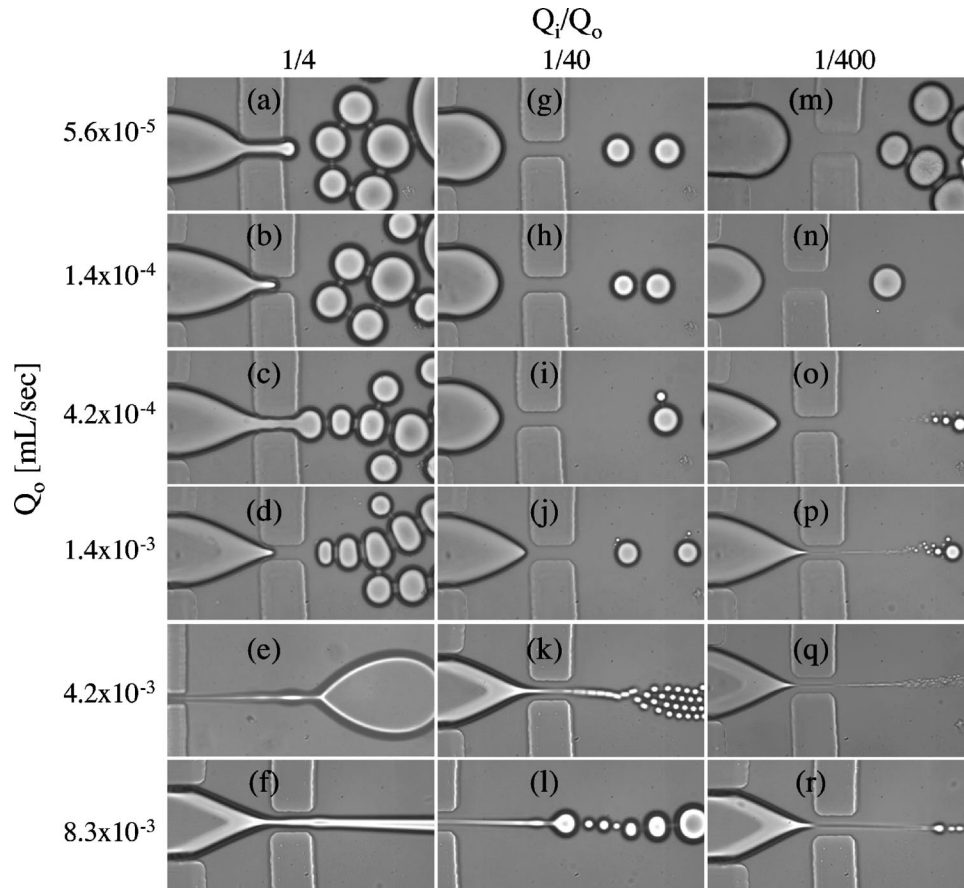

FIG. 3. Phase diagram for drop formation in flow focusing. Each image represents the drop sizes and drop patterns that form at the specified value of Q_o (rows) and Q_i/Q_o (columns). We note that for these flows the Reynolds numbers $\mathcal{R} = Q/(\nu h)$, where ν is the kinematic viscosity of the fluid and h is the height of the channel, of the oil (*o*) and water (*i*) are in the ranges $0.07 < \mathcal{R}_o < 12$ and $0.001 < \mathcal{R}_i < 18$, which are typically smaller than the values for the original flow-focusing studies (see Refs. 11 and 12).

monodisperse droplets over a range of flow rates in which the drop size is approximately the size of the orifice; see images (a)–(d), (g), and (m). In some cases coalescence occurs when droplets collide downstream of the orifice; see images (a)–(c) and (m). Such collisions can occur at low flow rates when the droplets cannot travel downstream quickly enough. Coalescence can, in principle, be reduced by appropriate use of surfactants to stabilize the droplets. For other conditions, generally corresponding to higher oil flow rates and lower ratios of Q_i/Q_o [images (h)–(j) and (n)–(p)], we observe bidisperse and polydisperse droplet distributions. Finally, the ability of the external fluid to form narrow threads of the inner fluid allows formation of monodisperse droplets with diameters much smaller than the orifice width [Figs. 3(k) and 3(q)], which is similar to the flow-focusing studies of Gañán-Calvo and co-workers.

In conclusion, we have integrated a flow-focusing configuration into a microchannel fabricated with soft lithography techniques. The operating diagram of drop size as a function of flow rate and flow rate ratios illustrates regimes with both monodisperse and polydisperse droplets. The smallest droplets produced can be much smaller than the orifice radius, in which case the drop size depends on the flow rates, and also there is a range of flow conditions where drops with diameters comparable to the orifice width are formed independent of the flow rates. In fact, we have fabricated an orifice approximately 10 μm in width, for which the smallest drop sizes observed are in the range of hundreds of nanometers. Drop formation with this configuration offers interesting possibilities for designing emulsions. Finally, it is worth noting that in these small devices wetting issues can be critical, as discussed recently by Dreyfus and co-workers.[16]

[1] C. Wibowo and K. M. Ng, AIChE J. **47**, 2746 (2001).
[2] T. Hamouda, M. M. Hayes, Z. Cao, R. Tonda, K. Johnson, D. C. Wright, J. Brisker, and J. R. Baker, Jr., J. Infect. Dis. **180**, 1939 (1999).
[3] S. Matsumoto, Y. Sugiyama, S. Sakata, and T. Hayashi, Liq. Cryst. **27**, 649 (2000).
[4] G. De Filpo, J. Lanzo, F. P. Nicoletta, and G. Chidichimo, J. Appl. Phys. **84**, 3581 (1998).
[5] P. Becher, *Emulsions: Theory and Practice* (Oxford University Press, Oxford, U.K., 2001).
[6] H. A. Stone and S. Kim, AIChE J. **47**, 1250 (2001).
[7] T. Thorsen, R. W. Roberts, F. H. Arnold, and S. R. Quake, Phys. Rev. Lett. **86**, 4163 (2001).
[8] V. Haverkamp, W. Ehrfeld, K. Gebauer, V. Hessel, H. Löwe, T. Richter, and C. Wille, Fresenius J. Anal. Chem. **364**, 617 (1999).
[9] M. W. Losey, M. A. Schmidt, and K. F. Jensen, Ind. Eng. Chem. Res. **40**, 2555 (2001).
[10] S. Sugiura, M. Nakajima, and M. Seki, Langmuir **18**, 2854 (2002).
[11] T. G. Mason and J. Bibette, Langmuir **13**, 4600 (1997).
[12] A. M. Gañán-Calvo and J. M. Gordillo, Phys. Rev. Lett. **87**, 274501 (2001).
[13] A. M. Gañán-Calvo, Phys. Rev. Lett. **80**, 285 (1998).
[14] J. C. McDonald, D. C. Duffy, J. R. Anderson, D. T. Chiu, H. Wu, O. J. A. Schueller, and G. M. Whitesides, Electrophoresis **21**, 27 (2000).
[15] G. M. Whitesides and A. D. Stroock, Phys. Today **54**, 42 (2001).
[16] R. Dreyfus, P. Tabeling, and H. Williams (unpublished).